Monthly Notices
of the
ROYAL ASTRONOMICAL SOCIETY

Mon. Not. R. Astron. Soc. **419,** 3109–3114 (2012) doi:10.1111/j.1365-2966.2011.19953.x

RXTE timing analysis of the anomalous X-ray pulsar 1E 2259+586

B. İçdem,[1] A. Baykal[1]★ and S. Ç. İnam[2]

[1]*Physics Department, Middle East Technical University, Ankara, Turkey*
[2]*Department of Electrical and Electronics Engineering, Başkent University, Ankara, Turkey*

Accepted 2011 October 4. Received 2011 September 30; in original form 2011 August 12

ABSTRACT

We present a pulse-timing analysis of *Rossi X-ray Timing Explorer* (*RXTE*) observations of the anomalous X-ray pulsar 1E 2259+586 from its 2002 outburst to 2010 October. We have the following objectives: to extend the work on the recovery stage after the 2002 glitch; to investigate the variations caused by the second glitch that occurred in 2007; to look for other unusual events, if any, that arise in the regular spin-down trend of the source. We find that the fractional change in the spin frequency derivative after the 2002 glitch is not stable as it decreased by an order of magnitude, from -2.2×10^{-2} to $-1.278(3) \times 10^{-3}$, in about 2.5 yr. Using a pulse-timing analysis, we discover two small frequency shifts with fractional changes $\Delta\nu/\nu = 3.08(32) \times 10^{-8}$ and $\Delta\nu/\nu = -1.39(11) \times 10^{-8}$. While the first of these shifts is not found to have a fractional frequency derivative change, the second has $\Delta\dot{\nu}/\dot{\nu} = -2.9(2) \times 10^{-2}$. We interpret these frequency changes as positive and negative microglitches, similar to those seen in radio pulsars.

Key words: pulsars: individual: 1E 2259+586 – X-rays: stars.

1 INTRODUCTION

The anomalous X-ray pulsar (AXP) 1E 2259+586 was discovered by Fahlman & Gregory (1981) within the supernova remnant G109.1–1.0 with ∼7 s pulsations. Further X-ray observations of 1E 2259+586 with *Tenma*, *EXOSAT* and *Ginga* (Koyama, Hoshi & Nagase 1987; Hanson et al. 1988; Morini et al. 1988; Koyama et al. 1989; Iwasawa, Koyama & Halpern 1992) have indicated that the AXP is steadily spinning down at a rate of $\dot{\nu} \sim -1.0 \times 10^{-14}$ Hz s^{-1}, which is too slow to power the observed X-ray luminosity. Using *ROSAT* observations, Baykal & Swank (1996) found a marginal spin-up episode between 1991 and 1992. Using *Rossi X-ray Timing Explorer* (*RXTE*) observations, Mereghetti, Israel & Stella (1998) have given an upper limit of 0.03 light-seconds for the semi-axis, suggesting a white-dwarf companion that is smaller than 0.8 $M_\odot$ (see also Baykal et al. 1998). Using *RXTE* observations, Kaspi, Chakrabarty & Steinberger (1999) have obtained, for the first time, a phase-coherent timing solution for 1E 2259+586 , indicating stability over a 2.6-yr time period. This stability strongly suggests a magnetar interpretation rather than the binary accretion hypothesis. Using *ASCA* and *BBXRT* observations, Corbet et al. (1995) have shown, for the first time, that the X-ray spectra can be explained by a blackbody plus power-law model. *INTEGRAL* and *RXTE* observations have revealed evidence of hard spectral tails above 10 keV (Kuiper et al. 2006; see also Kaspi & Boydstun 2010).

In 2002 June, 1E 2259+586 showed an outburst consisting of over 80 short soft gamma repeater (SGR)-like bursts (Gavriil, Kaspi & Woods 2004). During this outburst, the flux level of the source increased by a factor of more than 20, accompanied by a glitch of fractional frequency change $\Delta\nu/\nu \sim 4.24 \times 10^{-6}$ (Kaspi et al. 2003; Woods et al. 2004). In 2007, a second glitch of $\Delta\nu/\nu \sim 8.5 \times 10^{-7}$ was observed when the source was quiescent (Dib, Kaspi & Gavriil 2008).

Woods et al. (2004) modelled *XMM* and *RXTE* spectra of 1E 2259+586 before and after the 2002 outburst with the blackbody plus power-law model modified by interstellar absorption. The blackbody temperature increased rapidly after the outburst in contrast to the photon index, which decayed to about half of its pre-outburst value. Both parameters quickly recovered to within 25 per cent of their their pre-burst levels within the first ∼1–3 d (Woods et al. 2004). In the first few hours of the outburst, *XMM* and *RXTE* observations revealed that pulsed fraction decreased to ∼15 per cent, then, like the spectral parameters, it quickly recovered to its pre-outburst state within 6 d. There were also some variations in the phase dependence of the energy spectrum. While the photon index showed significant variability one week before the outburst, this variation vanished three days after the outburst. *XMM–Newton* observations of the source showed that the X-ray flux decayed with a power-law index of ∼−0.69 after the 2002 outburst until 2005. A strong correlation between the X-ray flux and hardness ratio has been observed by Zhu et al. (2008). The pulse profile of the source changed in such a way that much of the power moved to the fundamental harmonic and the second harmonic regained its power within one week, after which a very slow recovery was observed

★E-mail: altan@astroa.physics.metu.edu.tr

© 2011 The Authors
Monthly Notices of the Royal Astronomical Society © 2011 RAS

Downloaded from https://academic.oup.com/mnras/article-abstract/419/4/3109/2908051 by Middle East Technical University Library user on 24 July 2020

within several weeks (Woods et al. 2004). Using the cumulative properties of the outburst, Woods et al. (2004) concluded that the pulsar experienced something that was not sudden at all and included two components, one of which was on the surface (such as a series of fractures) and the other was distributed over a wider region smoothly. Hence, both the superfluid interior and the magnetosphere were affected.

The *Spitzer Space Telescope* observations of Kaplan et al. (2009) at the near- and mid-infrared regions of the electromagnetic spectrum have been interpreted as a possible indication of the presence of a passive X-ray-heated dust disc. Kaplan et al. (2009) have also shown that the infrared data of this source can also be modelled by a power-law spectrum, which can be explained by magnetospheric emission. Tian, Leahy & Li (2010) have estimated the distance to the AXP – and also to the supernova remnant (SNR) G109.1–1.0 – as 4.0 ± 0.8 kpc using the 21-cm H I-line and CO-line spectra of the SNR G109.1–1.0, the H II region Sh 152 and the adjacent molecular cloud complex.

In this paper, we construct phase-coherent pulse arrival times between 2002 and 2010. Using these arrival times, we refine the timing solution after the 2002 glitch and we look for frequency and derivative changes in these time intervals.

2 DATA AND ANALYSIS

2.1 Data

The data set used in this work consists of *RXTE* proportional counter array (PCA) observations of the AXP 1E 2259+586 covering the time between 2000 March (MJD 51613) and 2010 October (MJD 55483). The PCA operates in the energy range 2–60 keV using an array of five collimated xenon/methane multi-anode proportional counter units (PCUs). The instrument has a total effective area of $\sim$6500 cm^2 and a field of view of $\sim 1^\circ$ FWHM (Jahoda et al. 1996).

A total of 479 observations were used for the analysis presented here. The durations of the observations vary from 10.6 ks to 0.2 ks, most being greater than 1 ks. During the analysed *RXTE* PCA observations, the number of active PCUs varied between 1 and 4. Because of timing concerns, we used all the available layers of all PCUs in our analysis.

2.2 Pulse-timing analysis

The GoodXenonWithPropane or GoodXenon mode and event mode data were energy-selected (2–10 keV) for all xenon layers, and were binned with a 125-ms time resolution. The time values in the light curves were then corrected to the Solar system barycentre. We used the standard analysis tools for *RXTE* PCA data included in the FTOOLS package to obtain the light curves and to merge them into a single light curve, covering all of the interval mentioned above. In the extraction of the light curves, we removed all the outburst events in order to avoid sudden pulse profile changes. The light curves were folded at frequencies given by Woods et al. (2004). The time series was split into intervals of approximately the same duration, and each segment was folded with a quadratic ephemeris with the same frequency and frequency derivative, so that we obtained a pulse profile for each time interval, which is made up of 20 phase bins. Then, we switched to the harmonic representation of pulse profiles, as introduced by Boynton & Deeter (1985):

$$f(\phi) = F_0 + \sum_{k=1}^{10} F_k \cos k(\phi - \phi_k). \quad (1)$$

The template pulse is extracted from a longer time interval, at which glitch recovery has already taken place:

$$g(\phi) = \sum_{k=1}^{10} G_k \cos k(\phi - \phi_k). \quad (2)$$

Then, by cross-correlating the pulse profiles with the template pulse, we obtained the pulse arrival times, $\Delta\phi$. In order to see the effect of pulse profile changes in pulse timing, we also performed pulse timing using first and second harmonics independently. Our pulse arrival times were consistent within the 1σ level with 10 harmonic expansions of pulse profiles for 20 phase bins. This suggests that even if the pulse profile changes, the pulse phases are not effected. As a final check, we gave weight to all pulse harmonics using the variances of harmonics from all pulses. We applied the cross-correlation for the weighted pulses (or filtered pulses), and again we obtained the pulse arrival times as those of unweighted pulses in the 1σ confidence level. We concluded that pulse shape changes do not have any effect on pulse phases and pulse-timing analysis.

In the top panel of Fig. 1, it can be seen that the slope of the pulse arrival times changes after the first glitch. In the estimation of pulse arrival times, the spin-down rate of the source was kept fixed at the value before the glitch, which is $\dot{\nu} = -9.92 \times 10^{-15}$ Hz s^{-1}. By modelling the pulse arrival times lying after the first glitch using a first-order polynomial, with $\Delta\phi = \phi_0 + \delta\nu t$, the new pulse arrival times were obtained for the corrected pulse frequency, $\nu_0 + \delta\nu$. In the second panel of Fig. 1, it is clearly seen that the slope of the pulse arrival times is shifted again after MJD 54300. The shift in the pulse frequency is found by again using the method explained above, and new pulse arrival times are obtained after MJD 54300 by correcting the pulse frequency again. The third panel of Fig. 1, where we present the pulse arrival times for the corrected frequencies after the first and second glitches, shows that there are additional breaks in the pulse arrival time series around MJD 53750 and 54880 (see vertical dashed lines labelled B and E).

The first glitch is at MJD 52443.13 and was reported by Kaspi et al. (2003) to be accompanied by an outburst of many individual bursts. About 1360 d after the first glitch, at around MJD 53750, we resolved a small fractional frequency shift of $\Delta\nu/\nu = 3.08(32) \times 10^{-8}$. Phase-connected pulse arrival times after MJD 54300 indicate another glitch with a fractional frequency change of $\Delta\nu/\nu \sim 8.20(2) \times 10^{-7}$. This second glitch is consistent with the 1σ level given by Dib et al. (2008) in their paper reviewing AXP glitches. Moreover, around MJD 54880, we have observed another fractional frequency shift of $\Delta\nu/\nu = -1.39(11) \times 10^{-8}$ with $\Delta\dot{\nu}/\dot{\nu} = -0.029(2)$. All the glitch episodes in this work are presented in Fig. 1, and timing solutions are given in Tables 1 and 2.

For the first glitch, as described in Woods et al. (2004), the standard post-glitch relaxation models, which consist of single or multiple exponential relaxation terms (Alpar et al. 1984b), did not provide reasonable fits. An alternative model is the irregular model, including an exponential rise term, which has been developed for two glitches of the Crab pulsar (Lyne, Pritchard & Graham-Smith 1993; Wong, Backer & Lyne 2001). In this model, the increase in the slow-down rate is interpreted as the cumulation of successive glitches; part of the increase is provided by a step and part is in the form of an exponential rise

$$\nu = \nu_0 + \dot{\nu}_0(t - t_0) + \Delta\nu + \Delta\nu_g[1 - e^{-(t-t_g)/\tau_g}] - \Delta\nu_d[1 - e^{-(t-t_g)/\tau_d}] + \Delta\dot{\nu}t. \quad (3)$$

Downloaded from https://academic.oup.com/mnras/article-abstract/419/4/3109/2908051 by Middle East Technical University Library user on 24 July 2020

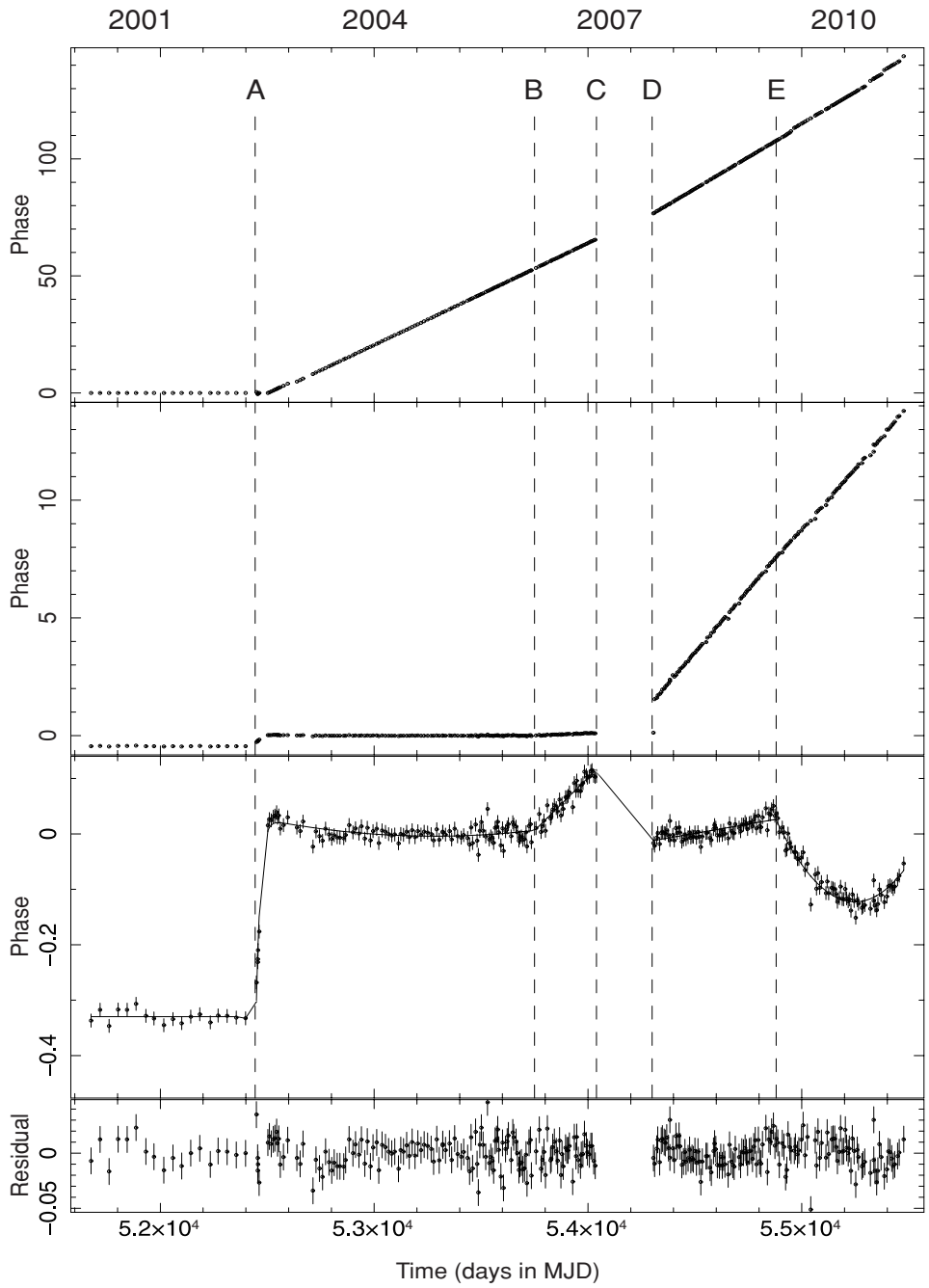


Figure 1. Phase-offset series for AXP 1E 2259+586. The panels are described from top to bottom. Top panel: phase offsets extracted using the spin-down model of the period before the 2002 glitch. Second panel: phase offsets using the correction of the pulse frequency after MJD 53443.13. Third panel: arrival times obtained by an additional correction after MJD 54300. The solid curve is the phase-offset evolution of the models presented in Tables 1 and 2. Bottom panel: the residuals, after subtracting the best-fitting models given in Tables 1 and 2. In all panels, the glitch epochs are indicated with dashed vertical lines: A, the 2002 glitch corresponds to MJD 52443.13; B, a small microglitch at MJD ∼53750; C–D, no phase connection; D, a second glitch at MJD ∼54300; E, a small microglitch at MJD ∼54880.

Here, the first two terms represent the frequency evolution before the glitch, t_g is the glitch epoch, $\Delta\nu$ is the frequency jump with the glitch, $\Delta\nu_g$ and $\Delta\nu_d$ are the growth and decay amplitudes, respectively, τ_g and τ_d are the growth and decay time- scales respectively, and $\Delta\dot{\nu}$ is the jump in the spin-down rate. We used the corresponding phase evolution equation to fit our pulse arrival times in the period MJD 52390–53750. (The correction to the pulse frequency after the first glitch mentioned above is $\delta\nu = \Delta\nu + \Delta\nu_g - \Delta\nu_d$.) In the fitting process, we use the χ^2 statistic and leave all parameters as free parameters. For normalizations of exponentials, we used the initial ranges as given by Woods et al. (2004).

In Table 1, we present timing solution of the first glitch for the extended time coverage from MJD 51613 to MJD 53750. Our analysis indicates that $\Delta\dot{\nu}/\dot{\nu}$ has shown a variation from -2.2×10^{-2} to $-1.278(3) \times 10^{-3}$ (i.e. there is an order of magnitude reduction in the fraction in a ∼2.5-yr time period). We have also

© 2011 The Authors, MNRAS **419,** 3109–3114
Monthly Notices of the Royal Astronomical Society © 2011 RAS

Downloaded from https://academic.oup.com/mnras/article-abstract/419/4/3109/2908051 by Middle East Technical University Library user on 24 July 2020

Table 1. Timing solution for 1E 2259+586 before MJD 53750. Numbers in parentheses indicate the 1σ uncertainties in the least significant digits quoted.

Parameter	Value[a]	Value[b]
Spin frequency, ν (Hz)	0.14328703257(21)	0.14328703257(21)
Spin-frequency derivative, $\dot{\nu}$ (Hz s^{-1})	$-9.920(6) \times 10^{-15}$	$-9.920(6) \times 10^{-15}$
Epoch (MJD)	52400	52400
$\Delta\nu$ (Hz)	$5.25(12) \times 10^{-7}$	$6.70(1.14) \times 10^{-7}$
$\Delta\nu_{\rm g}$ (Hz)	$>8.7 \times 10^{-7}$	$8.29(78) \times 10^{-7}$
$\tau_{\rm g}$ (d)	14.1(7)	14.1(1.2)
$\Delta\nu_{\rm d}$ (Hz)	$\Delta\nu_{\rm g} + (\sim 5 \times 10^{-9})$	$1.06(8) \times 10^{-6}$
$\tau_{\rm d}$ (d)	15.9(6)	15.9(1.1)
$\Delta\dot{\nu}$ (Hz s^{-1})	$2.18(25) \times 10^{-16}$	$1.268(3) \times 10^{-17}$
$t_{\rm g}$ (MJD)	52443.13(9)	52443.13(10)
Rms timing residual (ms)	44.9	85.1
Start observing epoch (MJD)	51613	51613
End observing epoch (MJD)	52900	53750

[a]Taken from table 4 of Woods et al. (2004).
[b]From our analysis.

Table 2. Timing solution for 1E 2259+586 after MJD 53750. Numbers in parentheses give the 1σ uncertainties in the least significant digits quoted.

Parameter	Microglitch 1	Glitch 2	Microglitch 2
Spin frequency, ν, (Hz)	0.143286381(13)	0.143286138(14)	0.143285760(14)
Spin-frequency derivative, $\dot{\nu}$ (Hz s^{-1})	$-9.920(6) \times 10^{-15}$	$-9.920(6) \times 10^{-15}$	$-9.920(6) \times 10^{-15}$
Epoch (MJD)	53750	54040	54880
$\Delta\nu$ (Hz)	$4.42(46) \times 10^{-9}$	$>1.6 \times 10^{-6}$	$-2.00(15) \times 10^{-9}$
$\Delta\dot{\nu}$ (Hz s^{-1})	–	–	$2.91(22) \times 10^{-16}$
$t_{\rm g}$ (MJD)	∼53750	∼54040	∼54880
Rms timing residual (ms)	76.8	66.8	106.7
Start observing epoch (MJD)	53700	53900	54800
End observing epoch (MJD)	54040	54900	55570

fitted the pulse arrival times for the time interval given by Woods et al. (2004), and we have found that the timing solution is consistent with Woods et al. (2004) at the 1σ level.

The small frequency shifts of $\Delta\nu/\nu \sim 10^{-8}$ with both signs at MJD 53750 and 54880 are of the order of microglitches seen in radio pulsars. In the first frequency shift, $\Delta\dot{\nu}/\dot{\nu}$ is not significant. However, in the second frequency shift, this value is found to be $-0.029(2)$ (i.e. the fractional change in the pulse-frequency derivative is negative). This is not very unusual when compared to the microglitches in radio pulsars, because there is no preferred sign for both fractional jumps $\Delta\nu/\nu$ and $\Delta\dot{\nu}/\dot{\nu}$ (Chukwude & Urama 2010). The timing parameters of these small frequency shifts are given in Table 2.

3 DISCUSSION

In this paper, we present the extended pulse-timing analysis of 1E 2259+586 from 2002 to 2010. In phase-coherent pulse-timing analysis, we have found that after the 2002 glitch $\Delta\dot{\nu}/\dot{\nu}$ reduced by an order of magnitude in a ∼2.5-yr time period. We have also discovered two microglitches $\Delta\nu/\nu = 3.08(32) \times 10^{-8}$ and $\Delta\nu/\nu = -1.39(11) \times 10^{-8}$. In the first frequency shift, we do not resolve the frequency derivative. In the second frequency shift, the fractional change in the spin-down rate is found to be $\Delta\dot{\nu}/\dot{\nu} = -2.9(2) \times 10^{-2}$.

Microglitches are a class of small amplitude resolvable jumps, which can be observed in both, or either of, the pulsar rotation frequency or its first time derivative (Cordes & Downs 1985; Cordes, Downs & Krause-Polstorff 1988; D'Alessandro et al. 1995; Chukwude 2002). The orders of magnitude for ν and $\dot{\nu}$ are in the range of $10^{-11} < |\Delta\nu/\nu| < 10^{-8}$ and $10^{-5} < |\Delta\dot{\nu}/\dot{\nu}| < 10^{-2}$, respectively. So far, 319 microglitches have been observed from 46 radio pulsars (Cordes & Downs 1985; D'Alessandro et al. 1995; Chukwude & Urama 2010). The microglitches observed in 1E 2259+586 are of the order of the upper limits of radio pulsar microglitches in magnitude . Unlike large glitches, microglitches can have both negative and positive signs in their fractional pulse frequencies and first time derivatives. Hence, it is difficult to understand microglitches in terms of the theories developed for large glitches (Cordes & Downs 1985; Cordes et al. 1988). The cause of microglitches is unclear but can be explained as involving neutron star interior and/or magnetospheric torque fluctuations (Ruderman, Zhu & Chen 1998). The magnetar crust can be cracked by the variations of the magnetic field configuration (Ruderman et al. 1998). In this case, both signs of microglitches might be observed.

Antiglitch (negative glitch) behaviour has been seen in two other magnetars (Thompson et al. 2000; Gavriil, Dib & Kaspi 2011). The sudden spin-down trend of SGR 1900+14 is interpreted by Thompson et al. (2000) as an antiglitch with a fractional pulse-frequency change of $\Delta\nu/\nu \sim 10^{-4}$. However, the scale of this event is four orders of magnitude larger than that of the negative microglitch of 1E 2259+586. For AXP 4U 0142+61, Gavriil et al. (2011) have shown that the total fractional frequency jump at the time of the glitch is $\Delta\nu/\nu \sim 1.7 \times 10^{-6}$; however, the decay of the large glitch event left a net negative slow-down portion of $\Delta\nu/\nu \sim -8 \times 10^{-8}$ after 17 d of recovery. In addition, for the rotation-powered pulsar PSR J1846–0258, Livingstone, Kaspi & Gavriil (2010) reported a

Downloaded from https://academic.oup.com/mnras/article-abstract/419/4/3109/2908051 by Middle East Technical University Library user on 24 July 2020

large spin-up glitch, which experienced a large recovery and ended up with a net decrease of pulse frequency similar to the recovery of AXP 4U 0142+61 and the event that occurred in SGR 1900+14. So far, among AXPs and SGRs, 1E 2259+586 is the only source to show microglitch/antiglitch events (Dib et al. 2008).

In magnetars, glitches might be triggered by strong internal magnetic fields as the crust is deformed, either plastically or cracking violently (Thompson & Duncan 1996). There might be some parts of the superfluid that are rotating more slowly than the crust. Then, with a glitch the angular momentum is transferred from the crust to the superfluid, in contrast to the case in radio-pulsar glitches, and the crust spins down after the glitch. This explanation has been proposed by Thompson et al. (2000) to explain the net spin-down rate event in SGR 1900+14. Hence, small-scale magnetar glitches can be used to explain the glitch/antiglitch trend of microglitches such as those seen in 1E 2259+586.

The 2002 glitch has been studied in depth by Woods et al. (2004) until the post-glitch recovery in mid-2003. We have extended the post-glitch recovery until the first microglitch event seen in 2006. In the pulse-timing analysis, we have confirmed that the fractional frequency change of the glitch has an amplitude of $\Delta\nu/\nu = 4.68(80) \times 10^{-6}$, and other post-glitch parameters (see Table 1) determined by Woods et al. (2004) from the observations with a time-span of 500 days. The fractional change in the pulse-frequency derivative $\Delta\dot{\nu}/\dot{\nu} = -1.278(3) \times 10^{-3}$, from our 1360-d pulse arrival times is found to be 17 times smaller than that of Woods et al. (2004), which was deduced from a shorter time interval. We should note that our analysis in their timing interval yielded a similar value in the 1σ limit. (This 1σ consistency in $\Delta\dot{\nu}/\dot{\nu}$ does not change even if we freeze the normalizations of the exponential components to the values given by Woods et al. 2004.) This indicates that the fractional change of the pulse-frequency derivative is variable. As discussed by Woods et al. (2004), the negative sign of the fractional change of the pulse-frequency derivative is unusual for large radio pulsar glitches. For large glitches, the fractional frequency change is $\Delta\nu/\nu > 10^{-7}$ and the fractional pulse-frequency derivative has the range $\Delta\dot{\nu}/\dot{\nu} \sim 10^{-2}$–$10^{-3}$ (see also Alpar & Baykal 1994, 2006).

In the standard large glitches of radio pulsars, the sudden shifts in the pulse frequency and the spin-down rate of a radio pulsar have been considered to be a result of the coupling mechanism between the crust and the crust superfluid (Alpar et al. 1984a,b; Alpar, Cheng & Pines 1989). The angular momentum transfer between the crust superfluid and the crust is provided by the quantized vortices. There are two types of vortex lines, separated according to their dynamical behaviour in the superfluid. Vortices of the first type are responsible for the continuous vortex flow, because the vortex lines are not pinned to the inner crust of the neutron star but they unpin and repin at some rate. Vortices of the second type are pinned to the crustal nuclei and are not allowed to move radially outwards up to the maximum tolerance of the pinning force. Hence, a lag appears between the spin-down rates of the crust and the superfluid, $\nu = \nu_s - \nu_c > 0$. When the vortices can no longer sustain this lag, they suddenly unpin from the crustal nuclei and some angular momentum is transferred to the crust. This sudden unpinning of the superfluid neutron vortices from the crustal nuclei can result in glitches of the fractional pulse-frequency changes of $\Delta\nu/\nu \sim 10^{-7}$ to 10^{-6}, together with increases in the magnitudes of the spin-down rate. Vortices of the second type do not have any contribution to the usual spin-down trend of the pulsar other than the glitches. Hence, the relaxation of the spin-down rate after the glitch is accomplished by the continuous vortex flow, and the persistent change in the spin-down rate, which is sometimes observed, is interpreted as the increase in the amount of pinned vortices that cannot move towards the outer crust after the glitch. If the superfluid part supplying the vortex flow has a moment of inertia I_A and the trapped part has a moment of inertia I_B, then the equations governing the dynamics of the glitches are determined as follows (Alpar 1995):

$$\frac{\Delta\nu}{\nu} = \left(\frac{I_A}{2I} + \frac{I_B}{I}\right)\frac{\delta\nu}{\nu}; \tag{4}$$

$$\frac{\Delta\dot{\nu}}{\dot{\nu}} = \frac{I_A}{I}. \tag{5}$$

Here, I is the total moment of inertia of the pulsar and $\delta\nu$ is the change of the rotation frequency of the superfluid interior. Thus, in vortex creep theory, the fractional change in the spin-down rate is determined by the fraction I_A/I, which should have a positive value in the presence of a constant external torque applied to the pulsar. Unless the vortices propagate inwards to the rotation axis of the star, the negative value of $\Delta\dot{\nu}/\dot{\nu}$ can be explained by external torques. This could be a result of the secular change of the magnetic moment (Ruderman 1991) or a change in the electromagnetic torque by a reorganization of the magnetic moment and angular momentum axis of the star (Link & Epstein 1997). However, the fractional change of the pulse-frequency derivative by a factor of 17 in a time-scale of only 860 d because of the change in magnetic moment is quite fast. Another explanation could be the relaxation of twisted magnetic fields, which creates stresses on the crust (Thompson, Lyutikov & Kulkarni 2002). Persistent seismic activity might modulate the spin-down torque and crustal shear waves, driving particle wind and causing changes in angular momentum (Thompson & Blaes 1998; Harding, Contopoulos & Kazanas 1999; Thompson et al. 2000). It is interesting to note that all the glitches of 1E 2259+586 have occurred almost at a constant spin-down rate of $\dot{\nu} = -9.920 \times 10^{-15}\,\mathrm{Hz}^{-1}$. This suggests that the glitches occur when post-glitch frequency derivatives are completely relaxed. Therefore, the excitation of precession during the glitch, as a result of a stable reorientation of the magnetic axis relative to the rotation axis of the star, is considered to be unlikely because the long-term torque on the star is not stable (Link & Epstein 1997).

Finally, we note that after the 2002 glitch, Kaspi et al. (2003) reported $\Delta\dot{\nu}/\dot{\nu} \sim 1.1$ for a time-span of a couple of weeks. They have suggested that the increase of the spin-down rate is a result of the decoupling of the crust and core superfluid where they recouple in a two-week time-scale, which is extremely long compared to theoretical estimates (Alpar & Sauls 1988; Sidery & Alpar 2009). This is also clearly resolved in our pulse-timing analysis for a particular short time-span. However, as we are interested in new events in the long-term recovery and unusual events in pulse timing, this aspect of the 2002 glitch is ignored in this paper.

ACKNOWLEDGMENTS

We acknowledge the research project TBAG 109T748 of the Scientific and Technological Research Council of Turkey (TÜBİTAK). AB also appreciates useful discussions with M. Ali Alpar and K. S. Cheng, who commented on the paper. We thank an anonymous referee for the useful suggestions that have improved the paper.

REFERENCES

Alpar M. A., Pines D., Anderson P., Shaham J., 1984a, ApJ, 276, 325
Alpar M. A., Pines D., Anderson P., Shaham J., 1984b, ApJ, 278, 797
Alpar M. A., Baykal A., 1994, MNRAS, 269, 849

Downloaded from https://academic.oup.com/mnras/article-abstract/419/4/3109/2908051 by Middle East Technical University Library user on 24 July 2020

Alpar M. A., Baykal A., 2006, MNRAS, 372, 489
Alpar M. A., Cheng K. S., Pines D., 1989, ApJ, 346, 823
Alpar M. A., 1995, in Alpar M. A., Kizilõlu, van Paradijs J., eds, Proc. NATO ASI Series C Vol. 450, The Lives of Neutron Stars. Kluwer Academic, Dordrecht, p. 185
Alpar M. A., Sauls J. A., 1988, ApJ, 327, 723
Baykal A., Swank J., 1996, ApJ, 460, 470
Baykal A., Swank J. H., Strohmayer T., Stark M. J., 1998, A&A, 336, 173
Chukwude A. E., 2002, PhD thesis, University of Nigeria, Nsukka
Chukwude A. E., Urama J. O., 2010, MNRAS, 406, 1907
Corbet R. H. D., Smale A. P., Ozaki M., Koyama K., Iwasawa K., 1995, ApJ, 443, 786
Cordes J. M., Downs G. S., 1985, ApJS, 59, 343
Cordes J. M., Downs G. S., Krause-Polstorff J., 1988, ApJ, 330, 847
D'Alessandro F., McCulloch P. M., Hamilton P. A., Deshpande A. A., 1995, MNRAS, 277, 1033
Deeter J. E., Bonynton D. E., 1985, in Hayakawa S., Nagase F., eds, Proc. Inuyama Workshop on Timing Analysis of X-ray Sources. Nagoyo Univ. Nagoyo, p. 29
Dib R., Kaspi V. M., Gavriil F. P., 2008, ApJ, 673, 1044
Fahlman G. G., Gregory P. C., 1981, Nat, 293, 202
Gavriil F. P., Dib R., Kaspi V. M., 2011, ApJ, 736, 138
Gavriil F. P., Kaspi V. M., Woods P. M., 2004, ApJ, 607, 959
Hanson C. G., Dennerl K., Coe M. J., Davis S. R., 1988, A&A, 195, 114
Harding A. K., Contopoulos I., Kazanas D., 1999, ApJ, 525, L125
Iwasawa K., Koyama K., Halpern J. P., 1992, PASJ, 44, 9
Jahoda K., Swank J. H., Giles A. B., Stark M. J., Strohmayer T., Zhang W., Morgan E. H., 1996, in Siegmund O. H., Gummin M. A., eds, Proc. SPIE, 2808, 59
Kaplan D. L., Chakrabarty D., Wang Z., Wachter S., 2009, ApJ, 700, 149
Kaspi V. M., Boydstun K., 2010, ApJ, 710, L115
Kaspi V. M., Chakrabarty D., Steinberger J., 1999, ApJ, 525, L33
Kaspi V. M., Gavriil F. P., Woods P. M., Jensen J. B., Roberts M. S. E., Chakrabarty D., 2003, ApJ, 588, L93
Koyama K., Hoshi R., Nagase F., 1987, PASJ, 39, 801
Koyama K. et al., 1989, PASJ, 41, 461
Kuiper L., Hermsen W., den Hartog P. R., Collmar W., 2006, ApJ, 645, 556
Link B., Epstein R. I., 1997, ApJ, 478, L91
Livingstone M. A., Kaspi V. M., Gavriil F. P., 2010, ApJ, 710, 1710
Lyne A. G., Pritchard R. S., Graham-Smith F., 1993, MNRAS, 265, 1003
Mereghetti S., Israel G. L., Stella L., 1998, MNRAS, 296, 689
Morini M., Robba N. R., Smith A., van der Klis M., 1988, ApJ, 333, 777
Ruderman M., Zhu T., Chen K., 1998, ApJ, 492, 267
Ruderman R., 1991, ApJ, 382, 576
Sidery T., Alpar M. A., 2009, MNRAS, 400, 1859
Thompson C., Blaes O., 1998, Phys. Rev. D, 57, 3219
Thompson C., Duncan R. C., 1996, ApJ, 473, 322
Thompson C., Duncan R. C., Woods P. M., Kouveliotou C., Finger M. H., van Paradijs J., 2000, ApJ, 543, 340
Thompson C., Lyutikov M., Kulkarni S. R., 2002, ApJ, 574, 332
Tian W. W., Leahy D. A., Li D., 2010, MNRAS, 404, L1
Wong T., Backer D. C., Lyne A. G., 2001, ApJ, 548, 447
Woods P. M. et al., 2004, ApJ, 605, 378
Zhu W., Kaspi V. M., Dib R., Woods P. M., Gavriil F. P., Archibald A. M., 2008, ApJ, 686, 520

This paper has been typeset from a TEX/LATEX file prepared by the author.

Downloaded from https://academic.oup.com/mnras/article-abstract/419/4/3109/2908051 by Middle East Technical University Library user on 24 July 2020